Geophysical Research Letters
DEC 12 2006; 33 (23) NIL_39-NIL_43
http://dx.doi.org/10.1029/2006GL027157

An edited version of this paper was published by AGU.

Role of bathymetry in Agulhas Current configuration and behaviour

S. Speich[1], J. R. E. Lutjeharms[2], P. Penven[3,4] and B. Blanke[1]

[1] Laboratoire de Physique des Océans, UMR 6523, Unité de Formation et de Recherche Sciences, Université de Bretagne Occidentale, Brest, France
[2] Department of Oceanography, University of Cape Town, Rondebosch, South Africa
[3] Institut de Recherche pour le Développement, Centre de Brest
[4] Institut Français de Recherche pour l'Exploitation de la Mer, Plouzané, France

Abstract:

The Agulhas Current forms an important link in the global ocean thermohaline circulation by its role in the inter-ocean exchange of water south of Africa. This process of ring shedding at the current's retroflection is dependent on perturbations to its trajectory that are sensitive to bathymetry. These perturbations may furthermore force the current to intersect shallow regions resulting in substantial changes to its path. A number of other flow characteristics of the system have also been deemed to be influenced by bathymetry. How dependent is Agulhas Current behaviour therefore on the bottom topography? We have used a regional, primitive equation model for initial experimentation. Removing the Agulhas Bank leads to enhanced inter-ocean flux, indicating its importance for inter-ocean exchange. Excising the Agulhas Plateau causes meridional meanders in the Agulhas Return Current to be unlocked from the bathymetry. Smoothing the continental slope weakens the current and substantially increases the direct inter-ocean flux.

1. Introduction

The Agulhas Current (AC in the following) is a major western boundary current along the south-east coast of Africa. South of the continent it retroflects and most of its water subsequently becomes part of the Agulhas Return Current [*Lutjeharms and Ansorge*, 2001] that carries out large meridional meanders on its way eastward. The retroflection of the AC is unstable and creates large Agulhas rings by loop occlusion. This is the prime mechanism by which warm and salty water from the Indian Ocean is transferred to the South Atlantic Ocean [*Gordon*, 1986]. Ring spawning events may be induced by the shedding of a lee eddy from the western side of the Agulhas Bank or by the arrival of a Natal Pulse [*Van Leeuwen et al.*, 2000], a singular meander, from far upstream. A well-developed Natal Pulse may even cause an upstream retroflection [*Lutjeharms and van Ballegooyen*, 1988] that will prevent AC water from reaching the normal retroflection location thus temporarily interrupting inter-ocean exchange. All these flow features are in some way dependent on the bathymetry.

It has been shown that the generation of Natal Pulses is due to an anomalously weak continental slope [*De Ruijter et al.*, 1999a] at the Natal Bight. When this meander precipitates an early retroflection, this is due to the current being forced across shallower topography of the Agulhas Plateau (location: see Figure 1). The disposition of the retroflection itself may be a function of the shape of the Agulhas Bank [*De Ruijter et al.*, 1999b] as is the presence of a lee eddy on its western side. The meridional meanders in the Agulhas Return Current in turn are thought to be forced by the shallow topography of the Agulhas Plateau [*Lutjeharms and van Ballegooyen*, 1984] and by the poleward extension of the Mozambique Plateau [*Gründlingh*, 1977]. The sensitivity of the AC to the bathymetry has also been indicated by modelling [e.g. *Lutjeharms and Webb*, 1995; *Matano*, 1996]. We have therefore experimented by removing certain key components of the bottom topography in a more refined model to see how the current configuration would react and thus to establish the importance of each of these components to the normal current configuration.

2. The regional model

Our circulation model is based on the IRD-UCLA version of the Regional Ocean Modelling System (ROMS) [*Shchepetkin and McWilliams*, 2003; 2005 ; *Penven et al.*, 2005]. The model domain extends from 5.8°E to 34°E and from 25.4°S to 44°S (Fig. 1). The model grid is 168×136 points with a resolution of 1/6° corresponding to a mean grid spacing of 12 km, which resolves the first baroclinic Rossby radius of deformation here (about 30 km, *Chelton et al.*, 1998). The grid is isotropic and does not introduce any asymmetry in the horizontal dissipation of turbulence. Therefore, it allows a fair representation of mesoscale dynamics. The bottom topography is derived from a 2' resolution database [*Smith and Sandwell*, 1997]. Although a new pressure gradient scheme associated to a specific equation of state limits errors in the computation of the pressure gradient (Shchepetkin and McWilliams, 2003a), the bathymetry has been filtered in order to keep a "slope parameter" (Beckmann and Haidvogel , 1993) $r = \frac{\Delta h}{2h} = \frac{h^{+1/2} - h^{-1/2}}{H^{+1/2} + H^{-1/2}} \leq 0.3$ for the control run (and smaller for a higher topographic smoothing).

The model has 32 vertical levels and the vertical s-coordinate is stretched for boundary layer resolution. All the model external forcing functions are derived from climatologies. At the surface, the model heat and fresh water fluxes are extracted from the COADS climatology [*Da Silva et al.*, 1994]. For the wind stress, a monthly mean climatology is computed from QuikSCAT scatterometer data. At the four lateral boundaries an active, implicit, upstream-biased, radiation condition connects the model solution to the surroundings [*Marchesiello et al.*, 2001]. In the case of inflow, the solution at the boundary is nudged toward a climatological velocity field calculated from the OCCAM 1/4° global ocean model that is also used as initial condition. All the simulations discussed in this manuscript were run for 11 years and model outputs were averaged and stored every 5 days of simulation.

3. Results

The results of four runs of the model are given here. These are a control run with fully intact bathymetry, a run without the Agulhas Bank, a run without the Agulhas Plateau and a run with a much smoothed shelf. Results from the control run are given in Figure 1.

The sea surface temperatures in this figure reproduce the known characteristic flow patterns of the region with a high degree of verisimilitude. The AC appears as a narrow ribbon at the shelf edge of the east coast with surface temperatures exceeding 26 ºC and an annual mean volume flux to the sea bottom at 30º E of 75 Sv (Sv = 10^6 m^3/s) [viz. *Beal and Bryden*, 1999]. South-west of the tip of Africa it retroflects. North-west of this retroflection there is evidence for a newly shed Agulhas ring (named A in Fig. 1a) while between these is an equatorward moving filament of cold, subantarctic water with a temperature of less than 14 ºC [viz. *Lutjeharms and Fillis*, 2003]. The frequency of ring shedding events in the model is realistic at about 4 per year [viz. *de Ruijter et al.*, 1999b]. The meridional meander of the Agulhas Return Current over the Agulhas Plateau is clearly circumscribed. Eddies shed by this meander move westward [*Boebel et al.*, 2003a]. South of this meander there is a warm

Agulhas eddy [*Lutjeharms*, 1987] that has entered the subantarctic zone (named B in Fig. 1a). Even a number of smaller features are well-represented. These include upwelling inshore of the current at the eastern extremity of the Agulhas Bank [*Lutjeharms et al.*, 2000], a cyclonic lee eddy west of this part of the shelf (named C in Fig. 1a) [*Penven et al.*, 2001a] and an AC filament [*Lutjeharms and Cooper*, 1996] being drawn equatorward in the South Atlantic. The altimetric results show a number of circulation features even more clearly.

In Figure 1b, the anti-cyclonic nature of the southern AC system stands out (warm colours). The meander over the Agulhas Plateau is again well-represented as is the retroflection extending to about 16º E on this occasion. A newly spawned Agulhas ring is evident in the Cape Basin to the west of the subcontinent as are a number of weaker remnants of rings all moving in a north-westward direction [*Schouten et al.*, 2000]. Some split, amalgamate with other rings or interact with cyclones [*Boebel et al.*, 2003b] that move in a south-westward direction. The lee eddy west of the Agulhas Bank is particularly prominent and is often seen to cut through the retroflection loop [*Lutjeharms et al.*, 2003] thus synchronised with a ring shedding event.

To evaluate the Indo-Atlantic inter-ocean exchange we made use of the ARIANE off-line Lagrangian diagnostic [http://univ-brest.fr/lpo/ariane; e.g. *Blanke et al.*, 1999]. Inter-ocean transport is then computed by releasing 140,000 virtual particles across a zonal section of the AC at 32°S in the Indian Ocean. and by integrating their individual trajectories and related infinitesimal transport forward in time till they reach defined final sections. These vertical sections completely close the modelled area and are located in the Atlantic, Southern Ocean and Indian sectors of the regional domain (Fig. 1c). Each trajectory is computed offline and integrated sequentially on the 5-day mean fields of the simulation. The virtual particles are released starting from year 4 of the simulation. We stop the deployment at year 8 allowing to the last released particles a 3-year delay to exit the domain. At the end of the integration, only a very small percentage of particles are still in the domain (about 2%). The water mass transfer between the AC and the South Atlantic thus derived is, in the control run, 41 ± 2 Sv. The uncertainty on the mass transfers was estimated from the sensitivity of the mass transfer to the particular sampling period adopted for the storage of the model output. This represents 55% of the total AC transport computed at 32°S and it is at the very high end of estimates of such fluxes to date. This is probably due to two different factors. First, the regional modelled domain is relatively small and therefore the final sections for the Lagrangian integration that close the South Atlantic and Southern Ocean sectors are very close to the African continent and still embedded in the very turbulent regime of the Cape Basin. This could induce an overestimate of water transfer to the South Atlantic, while, in reality, as a result of different mesoscale interactions, part of this water recirculates back to the Indian Ocean. Indeed, the Agulhas water flux that crosses the Atlantic section north of 35°S is only 25.4 ± 1.2 Sv. The remaining 15.6 ± 0.8 Sv of the computed leakage leave the Cape Basin with a south-west direction and reach the Atlantic final section south of 35°S. Second, the initial and open ocean boundary conditions are a monthly climatology derived from OCCAM, a global ocean model and not an observed climatology. Deviations of the mean thermohaline structure of OCCAM from observations could induce a difference in magnitude for the Indo-Atlantic connection.

The strong correspondence between these simulations and the known characteristics of the current system, as reflected in the cited literature, therefore gives us considerable confidence that this model incorporates the appropriate physics and captures the scales and the behaviour of the current adequately to experiment with the bathymetry. In the first experiment (Figure 2) the Agulhas Bank has been removed.

The most immediately striking aspect of this simulation is that the AC hugs the now zonal shelf edge south of Africa continuously. An excessive leakage of AC water into the South Atlantic of 56 ± 2.8 Sv takes place, (average for 8 model years) or 69% of the total. This large leakage appears also from the sea surface temperature structure (Figure 2a). A retroflective behaviour is present all the time, but the surface layers of the AC only take part in this about 46% of the time (viz. Figure 2b) usually moving directly west (Figure 2a). A lee eddy is formed on the western side of the land mass where the current overshoots, but is considerably more prominent than when the Agulhas Bank is present. This lee eddy passes south-westward between the ring and the new retroflection loop on 72% of the ring-shedding events (e.g. Figure 2a), more clearly seen in the sea surface height than in surface temperatures. We can only surmise if the movement of this eddy is opportunistic, when a gap appears between ring and retroflection, or is itself the cause of the ring shedding event. The location of the retroflection lies at least 3º of latitude further north than in the control run, but not further west. The latitude of the Subtropical Convergence remains virtually the same, at a mean of 42º S, making the retroflection loop much wider than normal. Meanders in the Agulhas Return Current are realistic and relatively stationary, whereas cold eddies shed from these meanders all move westward. An occasional leakage reminiscent of an upstream retroflection is seen. While the Agulhas Bank is almost completely removed, a small upwelling cell still exist inshore of the AC . Removal of the Agulhas Plateau leads to different current behaviour.

First, the behaviour of the Agulhas retroflection is much like that in the control run, including the location of the retroflection (not shown) and the average number of ring shedding events. However, the average volume transport of the AC is reduced to 66 Sv. This is due to the enormously reduced recirculation, and therefore of inertia and water entrainment, west of 32º E in the absence of the Agulhas Plateau. The mean Lagrangian flux into the South Atlantic is 34 ± 1.7 Sv. This value is lower than that for the control run, but still represents more than 50% of the total Agulhas transport at 32°S. The major change for this experiment is in the meanders in the Agulhas Return Current. When the topography is removed, non-stationary Rossby wave-like meanders forms as they are not anymore constrained to one geographic location as in the control run. They persistently move westward at about one degree of longitude in 11 (± 3.6) days.

The effects of reducing the steepness in the continental slope around southern Africa (by decreasing the "slope parameter" r to 0.1) are given in Figure 3. First, the surface speed of the AC is reduced from > 2 m/s in the control run to < 0.8 m/s with this smoothed slope (Figure 3). The current is wider and more diffuse. The intensity of the retroflection is much reduced with a considerable proportion of the current instead following the 1000 m isobath around the tip of Africa into the South Atlantic (Figure 3). The volume flux of the current is reduced to only 65 Sv in this experiment, but the percentage leakage into the South Atlantic is increased to 64%. The weaker the slope gradient, the less inertial the current is and the less will be the tendency to enter the South Atlantic as a free jet in a south-westerly direction and to retroflect. The propensity of the current core to continue to hold close to the shelf edge, well into the South Atlantic, may thus be increased, as is seen in Figure 3.

4. Conclusions

These preliminary modelling experiments show that the removal of certain prominent parts of the bottom topography at the AC termination has some important effects on the current's disposition. Removal of the Agulhas Bank leads to a substantial increase in the volume flux of the current into the South Atlantic and a seemingly increased role for a lee eddy off the west coast on the timing of ring shedding events. Excising the Agulhas Plateau leads to meridional meanders in the Agulhas Return Current moving steadily westward while the volume flux of the AC is reduced.

The sensitivity of the AC to bathymetry is particularly evident in experiments with the steepness of the shelf slope. Decreasing steepness leads to decreased speeds in the current, a less concentrated current and a greater tendency for it to move directly into the South Atlantic and not to form Agulhas rings.

The model we have used has a number of critical limitations. The one concerns the perennial quest for higher spatial resolution in models; the other the inadequacy of the boundary conditions. Both factors result in a lack of perturbations to the flow of the AC itself in the model. Such perturbations, in the form of the Natal Pulse, have been shown [e.g. *van Leeuwen et al.*, 2000] to be crucial to a proper understanding of the mechanisms responsible for inter-ocean exchange in the system. In order therefore to simulate the true situation better, improved model runs that include realistic mesoscale perturbations will doubtless improve these initial results.

Acknowledgements. This investigation was initiated during a visit by S. S. to the University of Cape Town in 2002 and completed during a visit by J. R. E. L. to the *Université de Bretagne Occidentale* in 2006. S. S. and J. R. E. L. thank the French

IRD for financial support for their reciprocal visits and S. S. acknowledges support from the French national programmes PATOM and PNEDC.

References

Beal, L. M. and H. L. Bryden (1999), The velocity and vorticity structure of the Agulhas Current at 32^o S, *J. Geophys. Res.*, *104*, 5151-5176.

Blanke, B., M. Arhan, S. Speich, and G. Madec (1999), Warm water paths in the equatorial Atlantic as diagnosed with a general circulation model, *J. Phys. Oceanogr.*, *29*, 2753–2768.

Boebel, O., T. Rossby, J. Lutjeharms, W. Zenk, and C. Barron (2003a), Path and variability of the Agulhas Return Current, *Deep-Sea Res. II*, *50*, 35-56.

Boebel, O., J. Lutjeharms, C. Schmid, W. Zenk, T. Rossby and C. Barron (2003b), The Cape Cauldron: a regime of turbulent inter-ocean exchange, *Deep-Sea Res. II*, 50, 57-86.

Chelton, D. B., R. A. de Szoeke, M. G. Schlax, K. E. Naggar, and N. Siwertz (1998), Geographical variability of the first-baroclinic Rossby radius of deformation, *J. Phys. Oceanogr.*, *28*, 433–460.

Da Silva, A. M., C. C. Young and S. Levitus (1994), Atlas of surface marine data 1994, vol. 1, algorithms and procedures, Tech. rep., U. S. Department of Commerce, NOAA.

De Ruijter, W. P. M., P. J. van Leeuwen and J. R. E. Lutjeharms (1999a), Generation and evolution of Natal Pulses: solitary meanders in the Agulhas Current, *J. Phys. Oceanogr.*, *29*, 3043-3055.

De Ruijter, W. P. M., A. Biastoch, S. S. Drijfhout, J. R. E. Lutjeharms, R. P. Matano, T. Pichevin, P. J. van Leeuwen and W. Weijer (1999b), Indian-Atlantic inter-ocean exchange: dynamics, estimation and impact, *J. Geophys. Res.*, *104*, 20,885-20,911.

Gordon, A. L. (1986), Inter-ocean exchange of thermocline water, *J. Geophys. Res.*, *91*, 5037-5046.

Gründlingh, M. L. (1977), Drift observations from Nimbus VI satellite-tracked buoys in the southwestern Indian Ocean, *Deep-Sea Res.*, *24*, 903-913.

Lutjeharms, J. R. E. (1987), Meridional heat transport across the Sub-Tropical Convergence by a warm eddy, *Nature*, *331*, 251-253.

Lutjeharms, J. R. E. and I. Ansorge (2001), The Agulhas Return Current, *J. mar. Syst.*, *30*, 115-138.

Lutjeharms, J. R. E. and R. C. van Ballegooyen (1984), Topographic control in the Agulhas Current system, *Deep-Sea Res.*, *31*, 1321-1337.

Lutjeharms, J. R. E. and R. C. van Ballegooyen (1988), Anomalous upstream retroflection in the Agulhas Current, *Science*, *240*, 1770-1772.

Lutjeharms, J. R. E. and D. J. Webb (1995), Modelling the Agulhas Current system with FRAM (*Fine Resolution Antarctic Model*), *Deep-Sea Res. I*, *42*, 523-551.

Lutjeharms, J. R. E. and J. Cooper (1996), Interbasin leakage through Agulhas Current filaments, *Deep-Sea Res. I*, *43*, 213-238.

Lutjeharms, J. R. E., J. Cooper and M. Roberts (2000), Upwelling at the inshore edge of the Agulhas Current, *Cont. Shelf Res.*, *20*, 737-761.

Lutjeharms, J. R. E. and C. S. Fillis (2003) Intrusion of sub-Antarctic water across the Subtropical Convergence south of Africa, *S. Afr. J. Sci.*, *99*, 173-176.

Lutjeharms, J. R. E., O. Boebel and T. Rossby (2003), Agulhas cyclones, *Deep-Sea Res. II*, *50*, 13-34.

Marchesiello, P., J. C. McWilliams and A. Shchepetkin (2001), Open boundary condition for long-term integration of regional oceanic models, *Ocean Model., 3*, 1–21, doi10.1016/S1463-5003(00)00013-5.

Matano, R. P. (1996), A numerical study of the Agulhas retroflection: the role of bottom topography, *J. Phys. Oceanogr.*, *26*, 2267-2279.

Penven, P., V. Echevin, J. Pasapera, F. Colas, and J. Tam (2005), Average circulation, seasonal cycle, and mesoscale dynamics of the Peru Current System: A modeling approach, *J. Geophys. Res*., *110*, C10021, doi:10.1029/2005JC002945.

Penven, P., J. R. E. Lutjeharms, P. Marchesiello, S. J. Weeks and C. Roy (2001a), Generation of cyclonic eddies by the Agulhas Current in the lee of the Agulhas Bank, *Geophys. Res. Lett.*, *28*, 1055-1058.

Penven, P., C. Roy, G. B. Brundrit, A. Colin de Verdière, P. Fréon, A. S. Johnson, J. R. E. Lutjeharms and F. A. Shillington (2001b), A regional hydrodynamic model of the Southern Benguela, *S. Afr. J. Sci.*, *97***,** 472 - 475.

Shchepetkin, A. F. and J. C. McWilliams (2005), The regional oceanic modeling system (ROMS): a split-explicit, free-surface, topography-following-coordinate oceanic model, *Ocean Model., 9*, 347–304, doi:10.1016/j.ocemod.2004.08.002.

Shchepetkin, A.F., McWilliams, J.C., 2003. A method for computing horizontal pressure-gradient force in an ocean model with a non-aligned vertical coordinate. Journal of Geophysical Research 108 (C3), 3090.

Schouten, M. W., W. P. M. de Ruijter, P. J. van Leeuwen and J. R. E. Lutjeharms (2000), Translation, decay and splitting of Agulhas rings in the south-eastern Atlantic ocean, *J. Geophys. Res.*, *105*, 21,913-21,925.

Smith, W. H. F., and D. T. Sandwell (1997), Global sea floor topography from satellite altimetry and ship depth soundings, *Science*, *227*, 1956–1962, doi:10.1126/science.277. 5334.1956.

Van Leeuwen, P. J., W. P. M. de Ruijter and J. R. E. Lutjeharms (2000), Natal Pulses and the formation of Agulhas rings, *J. Geophys. Res.*, 105, 6425-6436.

FIGURE CAPTIONS TO MS BY SPEICH ET AL.

Figure 1. Sea surface temperature distribution simulated for the southern Agulhas Current region on 3 March, model year 11 (**a**), with a temperature scale. Black lines show the bottom topography in km. The sea surface height in cm is given in panel (**b)**, for 28 December, model year 1. Note the locations of the Agulhas Bank and the Agulhas Plateau. (**c**) Interocean water mass transfer (with a 5-Sv C.I.) originating in the AC. The four sections of interception are also shown in red: "Agulhas current" (solid line), "Indian ocean" (dashed line), "Southern Ocean" (dotted line), and "Atlantic Ocean" (dash-dotted line).

Figure 2. The sea surface temperature distribution for the southern Agulhas Current region on 13 October, model year 4, when the Agulhas Bank has been removed (panel **a**). It shows a reduced retroflection. For 3 September, model year 4, (panel **b**) the retroflection is meridionally wide, but much better developed. Otherwise as in Figure 1.

Figure 3. The sea surface temperature for the Agulhas Current termination with a smoothed and weakened shelf slope. Otherwise as in Figure 1.

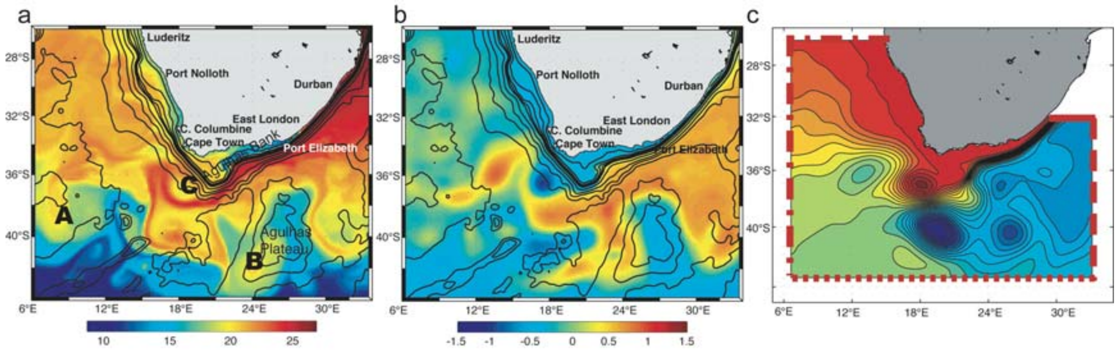

Figure 1. Sea surface temperature distribution simulated for the southern Agulhas Current region on 3 March, model year 11 (**a**), with a temperature scale. Black lines show the bottom topography in km. The sea surface height in cm is given in panel (**b)**, for 28 December, model year 1. Note the locations of the Agulhas Bank and the Agulhas Plateau. (**c**) Interocean water mass transfer (with a 5-Sv C.I.) originating in the AC. The four sections of interception are also shown in red: “Agulhas current” (solid line), “Indian ocean” (dashed line), “Southern Ocean” (dotted line), and “Atlantic Ocean” (dash-dotted line).

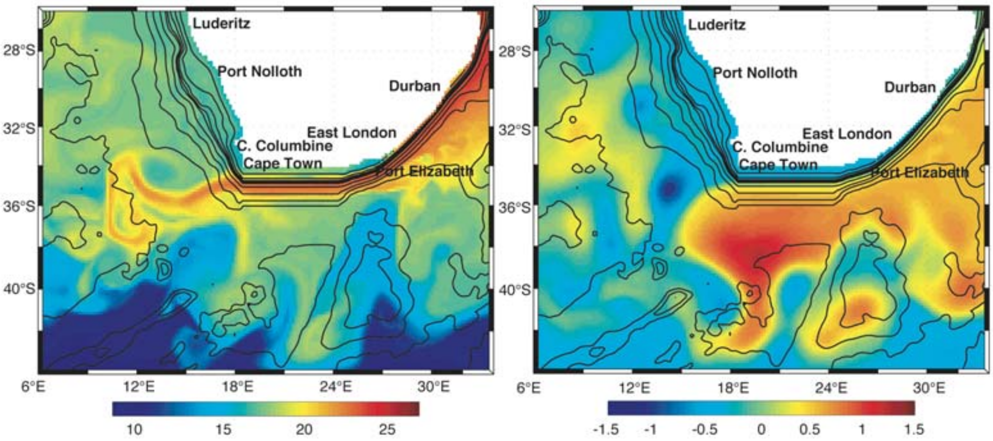

Figure 2. The sea surface temperature distribution for the southern Agulhas Current region on 13 October, model year 4, when the Agulhas Bank has been removed (panel **a**). It shows a reduced retroflection. For 3 September, model year 4, (panel **b**) the retroflection is meridionally wide, but much better developed. Otherwise as in Figure 1.

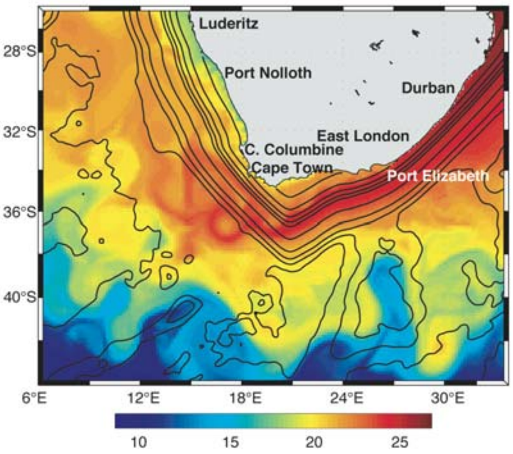

Figure 3. The sea surface temperature for the Agulhas Current termination with a smoothed and weakened shelf slope. Otherwise as in Figure 1.

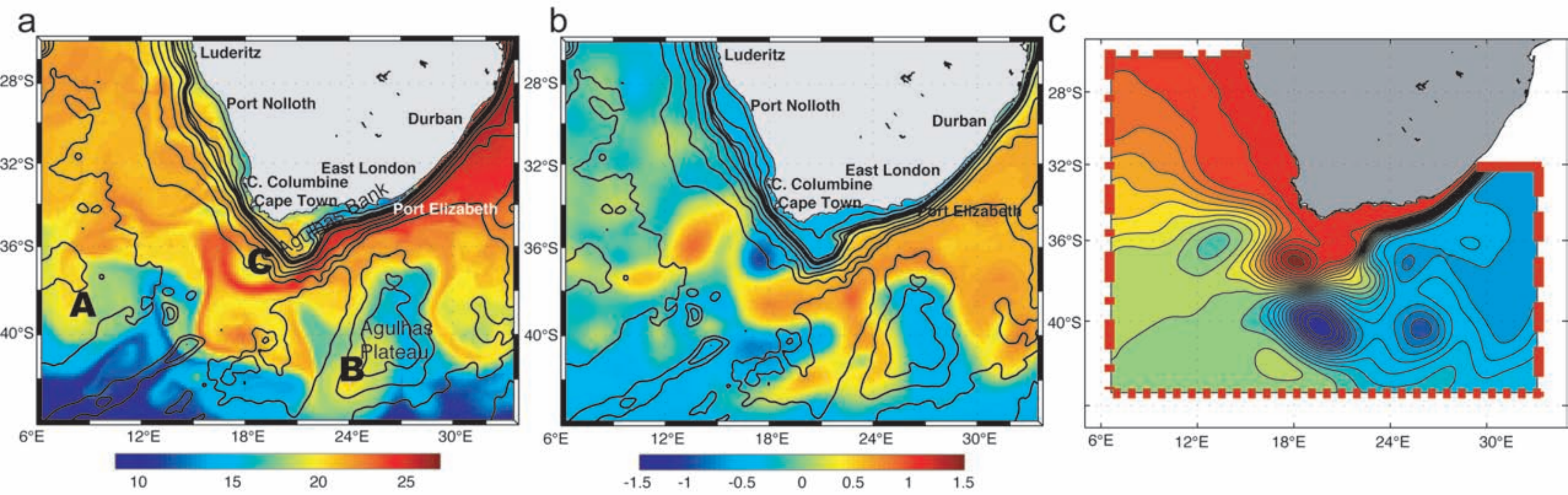
a
Luderitz
Port Nolloth
Durban
East London
C. Columbine
Cape Town
Agulhas Bank
Port Elizabeth
A
B
C
Agulhas Plateau
28°S
32°S
36°S
40°S
6°E
12°E
18°E
24°E
30°E
10
15
20
25
b
Luderitz
Port Nolloth
Durban
East London
C. Columbine
Cape Town
Port Elizabeth
28°S
32°S
36°S
40°S
6°E
12°E
18°E
24°E
30°E
-1.5
-1
-0.5
0
0.5
1
1.5
c
28°S
32°S
36°S
40°S
6°E
12°E
18°E
24°E
30°E

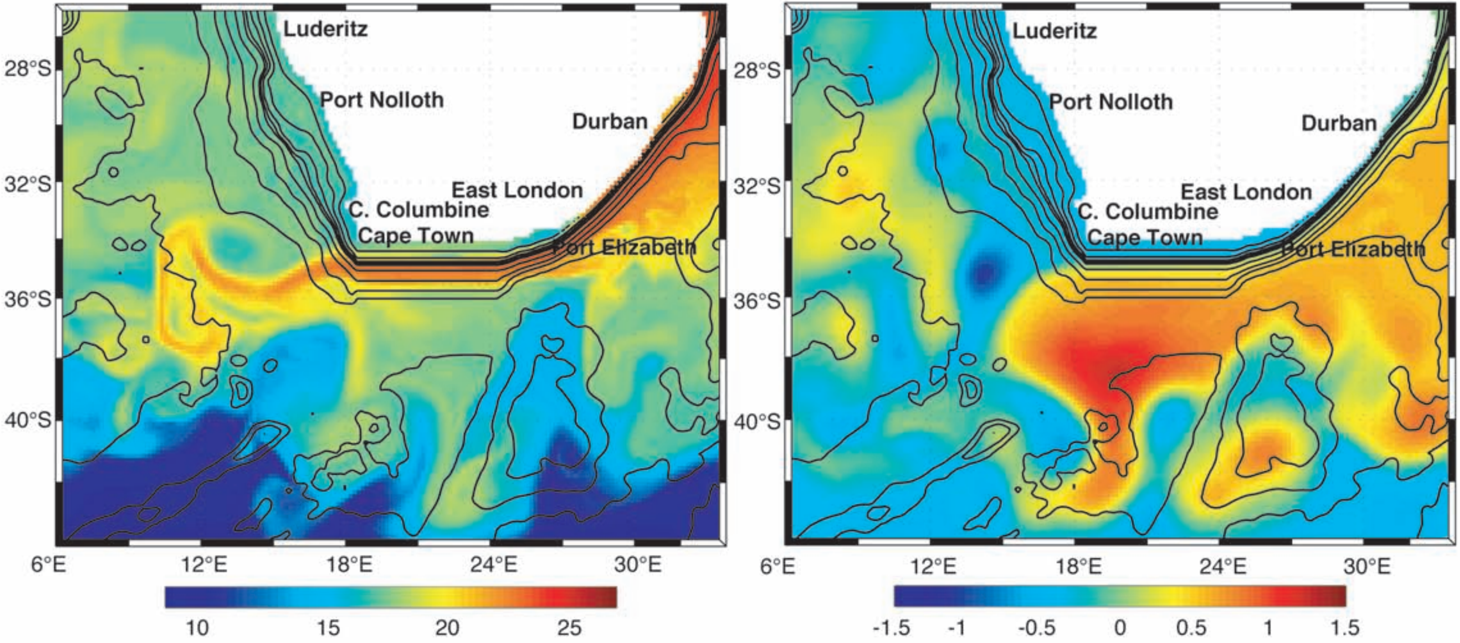

Luderitz
Port Nolloth
Durban
East London
C. Columbine
Cape Town
Port Elizabeth
28°S
32°S
36°S
40°S
6°E
12°E
18°E
24°E
30°E
10
15
20
25
Luderitz
Port Nolloth
Durban
East London
C. Columbine
Cape Town
Port Elizabeth
28°S
32°S
36°S
40°S
6°E
12°E
18°E
24°E
30°E
-1.5
-1
-0.5
0
0.5
1
1.5

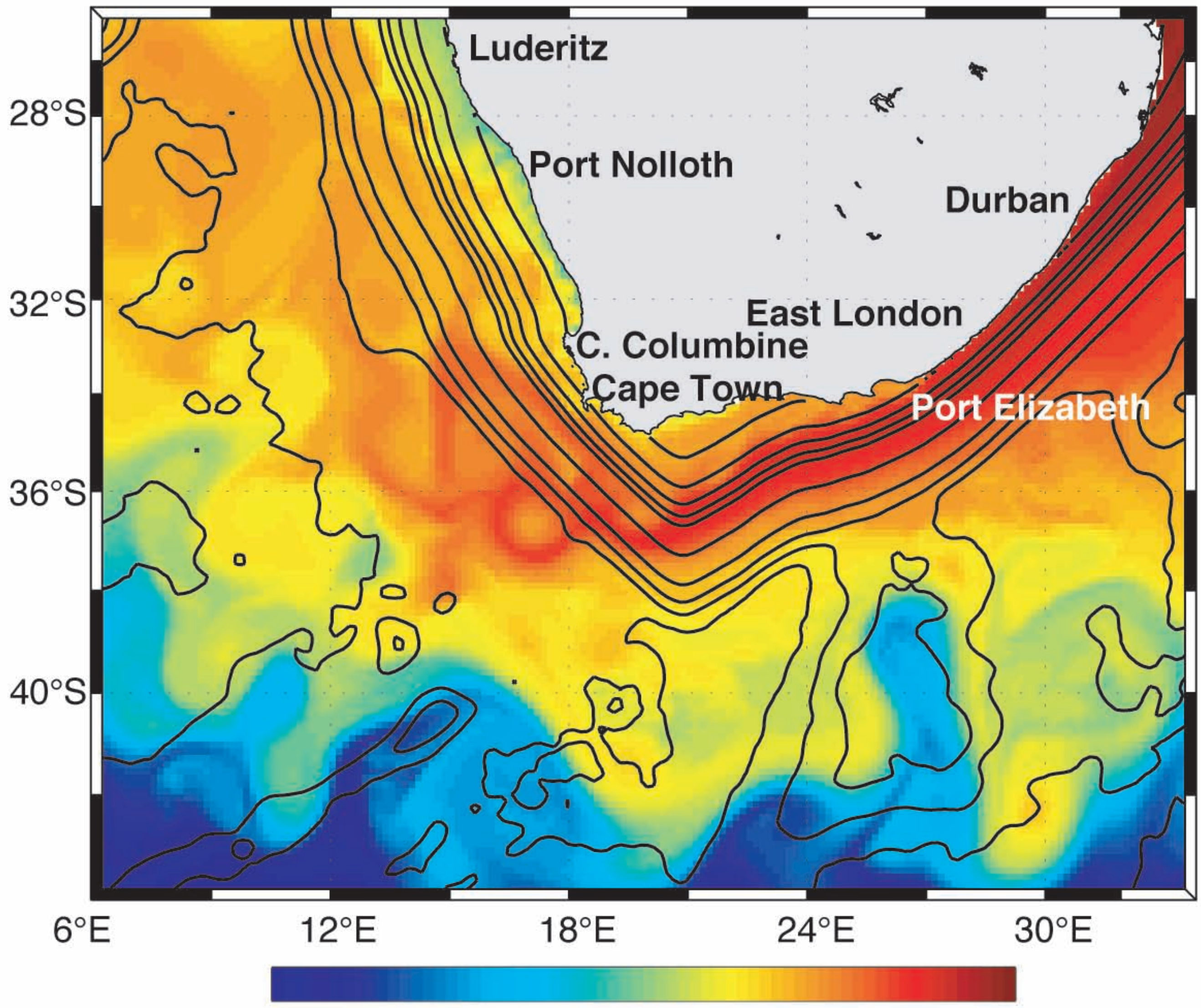
Luderitz
Port Nolloth
Durban
East London
C. Columbine
Cape Town
Port Elizabeth
28°S
32°S
36°S
40°S
6°E
12°E
18°E
24°E
30°E
10
15
20
25